

# A Novel Dual-Band Microstrip Bandstop Filter Based on Stepped Impedance Hairpin Resonators

Jangirkhan Dzhumamuhambetov<sup>1</sup>, Bakytgul Abykanova<sup>1</sup>, and Adnan Gorur<sup>2, \*</sup>

**Abstract**—In this paper, design of a novel dual-band microstrip bandstop filter is presented. The designed filter is constructed by loading two stepped impedance hairpin resonators to a simple straight transmission line, which also connects to the input and output ports. By virtue of the proposed resonator, the ratio of the first and second resonance frequencies can be obtained as approximately 4.4. Two stopbands centered at 2.34 GHz and 7.81 GHz with the fractional bandwidths of 33.2% and 7.9% can be obtained, respectively. Rejection levels inside the stopbands are better than 20 dB. Total electrical length of the proposed filter is  $0.317\lambda_g \times 0.136\lambda_g$ , where  $\lambda_g$  is the guided wavelength at the lowest resonance frequency. The designed filter was also fabricated and tested for experimental verification. The measured results are in an excellent agreement with the simulated ones.

## 1. INTRODUCTION

Bandstop filters are often used in many types of communication systems in order to suppress unwanted signals. Due to the rapid progress in modern communication systems, microwave filters having more than one passband or stopband have come into prominence. Therefore, there is an increasing demand for multi-band bandstop filter designs. For this purpose, several circuit types including microstrip, coplanar waveguides, and striplines can be utilized to obtain the desired frequency response. Among them, microstrip structures are used more than the others since they can provide design flexibility, low loss, low cost, etc. Using this information and approach, researchers try to design new microwave filters according to the different demands of different communication systems. Integration of the designed filter into any system is one of the important problems in the utilization of microwave filters. Therefore, simple structures are more preferred by users in order to integrate it to their system easily.

To date, multiband microstrip bandstop filters have been introduced in many approaches including composite resonators [1], open loop resonators [2], dual-mode loop resonators [3], stub loaded resonators [4], etc.. Additionally, hairpin resonators are not only used for microstrip bandstop filter design, but also used for any kind of microstrip filter design. Stepped impedance hairpin resonators are used to design compact and high performance lowpass filters in [5, 6]. In [5], the lowpass filter was formed by connecting a hairpin resonator to the input and output ports directly. This approach has also been developed by using cascaded stepped impedance hairpin resonators in order to increase the order of the lowpass filter [6]. Thus, selectivity of the filter could be increased. Hairpin resonators are mostly used in bandpass filter designs [7–12]. In [7], hairpin resonators have been introduced to the literature and a microstrip bandpass filter was designed. A narrow band bandpass filter with two transmission poles and multiple transmission zeros has been presented in [8]. Different kinds of hairpin resonators such as interdigital, short circuited and utilization in multiple layers have also been investigated to design various bandpass filters [9–11]. They have also been used to design ultra wideband microstrip

---

Received 24 February 2019, Accepted 22 May 2019, Scheduled 8 June 2019

\* Corresponding author: Adnan Gorur (adnangorur@hotmail.com).

<sup>1</sup> Department of Physics, Qazaqstan Atyrau State University, Atyrau, Kazakhstan. <sup>2</sup> Department of Electrical and Electronics Engineering, Niğde Ömer Halisdemir University, Niğde 51240, Turkey.

bandpass filters as introduced in [11] and [12]. In addition, hairpin resonators have been utilized in a microstrip bandstop filter in a similar approach with this paper. In [13], hairpin coupling structures have been used to satisfy compactness in a bandstop filter. On the other hand, a coupled line hairpin unit has been constructed by connecting two coupled lines with a high impedance transmission line [14]. Here, filter performance has also been improved by means of a defected ground structure located at the parallel coupled line section. Besides, a modified stepped impedance hairpin resonator has been used to design a dual-band bandstop filter [15]. Among hairpin resonators based bandstop filters, only one stopband can be obtained in [13] and [14]. In [15], although there were two stopbands, the measured results were poor.

In this paper, a novel dual-band bandstop filter is designed. For this purpose, firstly, a single stepped impedance hairpin resonator located to a simple straight transmission line is investigated. This transmission line also connects the input and output ports to each other. The proposed configuration allows two resonance frequencies, and the ratio of the resonance frequencies can be obtained approximately 4.4. In order to increase the filter order, one more identical hairpin resonator is added by increasing the length of the straight transmission line, and two stopbands can be obtained. Center frequencies of the stopbands are adjusted at 2.34 GHz and 7.81 GHz with fractional bandwidths of 33.2% and 7.9%, respectively. The designed filter was also fabricated and measured for the experimental verification. The measured results show an excellent agreement with the predicted ones. In the measured results, rejection levels have been obtained better than 20 dB for both stopbands. The designed dual-band bandstop filter allows a high center frequency ratio between the stopbands.

## 2. STEPPED IMPEDANCE HAIRPIN RESONATOR

The proposed stepped impedance hairpin resonator is depicted in Fig. 1(a). As can be seen from the figure, in order to emphasize the characteristics of the proposed resonator, it is connected to a simple straight transmission line which connects the input and output ports. Therefore, the proposed circuit can also be considered as a bandstop filter with a single pole. It should be noted that the transmission lines of the resonator are far away from each other so as to prevent extra coupling.

The equivalent half circuit models of the proposed resonator are illustrated in Figs. 1(b) and 1(c) for even and odd mode excitations, respectively. In Fig. 1(b), the even mode excitation is applied to

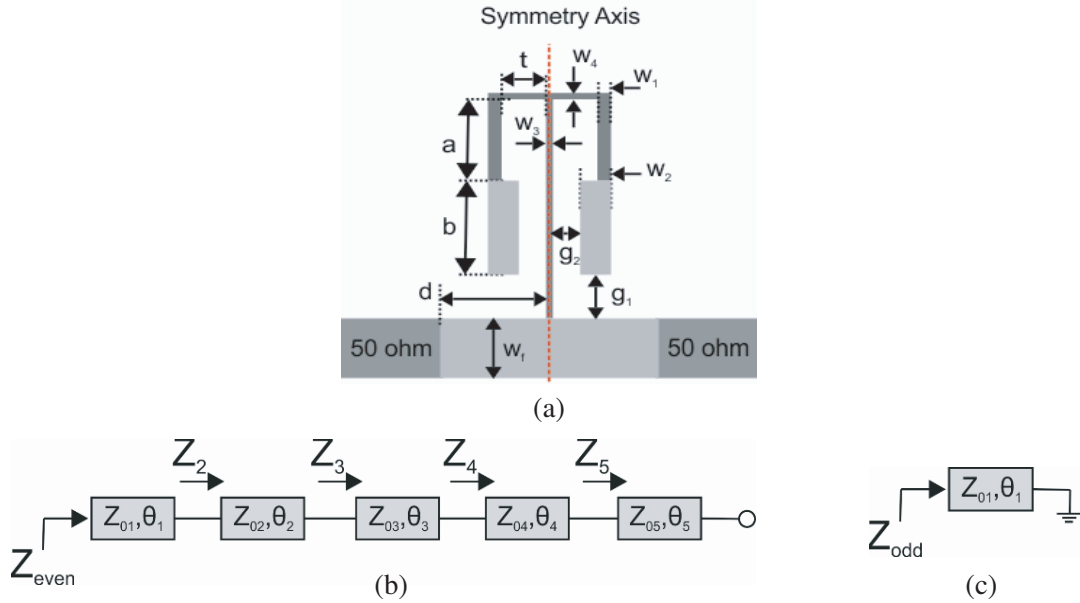


**Figure 1.** (a) Configuration of the proposed stepped impedance hairpin resonator, (b) even mode excitation, (c) odd mode excitation.

the circuit and the resonator is open-circuited at the symmetry axis. For the odd mode excitation, the resonator is short-circuited at the symmetry axis, as depicted in Fig. 1(c). According to Fig. 1(a), there are five transmission lines in the even mode half circuit model given in Fig. 1(b). Also, for the odd mode half circuit model, there is only one transmission line since the symmetry axis is short-circuited. The input impedances of transmission lines illustrated in Fig. 1(b) can be expressed as,

$$Z_n = Z_{0n} \frac{Z_L + jZ_{0n}\tan(\theta_n)}{Z_{0n} + jZ_L\tan(\theta_n)} \quad n = 2, 3, 4, 5 \quad (1)$$

where the impedance  $Z_L$  is the load impedance, and impedances  $Z_n$  and  $Z_{0n}$  are the input impedance and characteristic impedance of  $n$ th transmission line, respectively. In Eq. (1), for instance, the impedance  $Z_4$  can be found by taking  $Z_5$  instead of the load impedance  $Z_L$ . Also, the impedance  $Z_5$  is the input impedance of an open-circuited line and it can be expressed as,

$$Z_5 = -jZ_{05}\cot(\theta_5) \quad (2)$$

Thus, the even mode input impedance can be obtained by taking  $n = 1$  and the impedance  $Z_2$  as the load impedance in Eq. (1). So, it can be expressed as

$$Z_{even} = Z_{01} \frac{Z_2 + jZ_{01}\tan(\theta_2)}{Z_{01} + jZ_2\tan(\theta_2)} \quad (3)$$

The even mode resonance condition can be obtained by equating Eq. (3) to zero. From Fig. 1(c), the odd mode input impedance can be expressed as,

$$Z_{odd} = jZ_{01}\tan(\theta_1) \quad (4)$$

In the odd mode excitation, since the electrical length of the transmission line having the width of  $w_3$  is too small, it can be neglected. Again, the odd mode resonance condition can be obtained by equating Eq. (4) to zero.

The proposed resonator is simulated by a Full-Wave Electromagnetic Simulator [16]. In the design, an RT/Duroid substrate with a relative dielectric constant of 6.15 and a thickness of 1.27 mm was used. Dimensions shown in Fig. 1 are;  $a = 2.6$  mm,  $b = 3.0$  mm,  $w_1 = 0.4$  mm,  $w_2 = 0.9$  mm,  $w_3 = w_4 = 0.2$  mm,  $w_f = 1.9$  mm,  $d = 3.1$  mm,  $t = 1.3$  mm,  $g_1 = 0.4$  mm and  $g_2 = 0.8$  mm. Effects of  $w_1$  and  $w_4$  on the frequency response are depicted in Figs. 2(a) and 2(b). It is obvious that the increase in these widths decrease the total electrical length of the resonator. Thus, the second resonance frequency can be increased. In Fig. 2(a),  $w_1$  varies between 0.2 mm and 1.0 mm. It is clear that only the second resonance frequency can be changed, while the first one is fixed. From Fig. 2(a), ratio of the first and second resonance frequencies can be as high as approximately 4.4, while  $w_1$  is 1.0 mm. Fig. 2(b) shows the effects of  $w_4$  on the frequency response. The second resonance frequency can be controlled dramatically as compared to the first one. As a result of both of these figures, the second resonance frequency can be independently controlled. In addition, effects of  $w_3$  on the frequency response are also demonstrated in Fig. 2(c). In here, the first resonance frequency can be increased while  $w_3$  is increased, whereas the second resonance frequency exhibits opposite behaviour. Hence, the resonance frequencies of the stopbands are getting closer to each other depending on the increment in  $w_3$ . Those physical parameter investigations are useful to obtain the final circuit. According to Fig. 2, it should also be noted that there are three resonance frequencies. Thus, the proposed resonator can be considered for triple band bandstop filter design. However, the third resonance frequency cannot be independently controlled. Therefore, the proposed resonator should be considered more suitable for dual band bandstop filter designs, as explained here.

The ratio  $b/a$  has also remarkable effects on the frequency response as represented in Fig. 3. As can be seen from the figure, while the ratio  $b/a$  is increased, the first resonance frequency is decreased, but the second resonance frequency exhibits more different behaviour. Depending on the increment in the ratio  $b/a$ , the second resonance frequency firstly decreases and then begins increasing.

### 3. DUAL-BAND BANDSTOP FILTER DESIGN

Based on the above approaches, the design of a dual-band bandstop filter was achieved by using two stepped impedance hairpin resonators as shown in Fig. 4. Initial physical dimensions are adjusted at

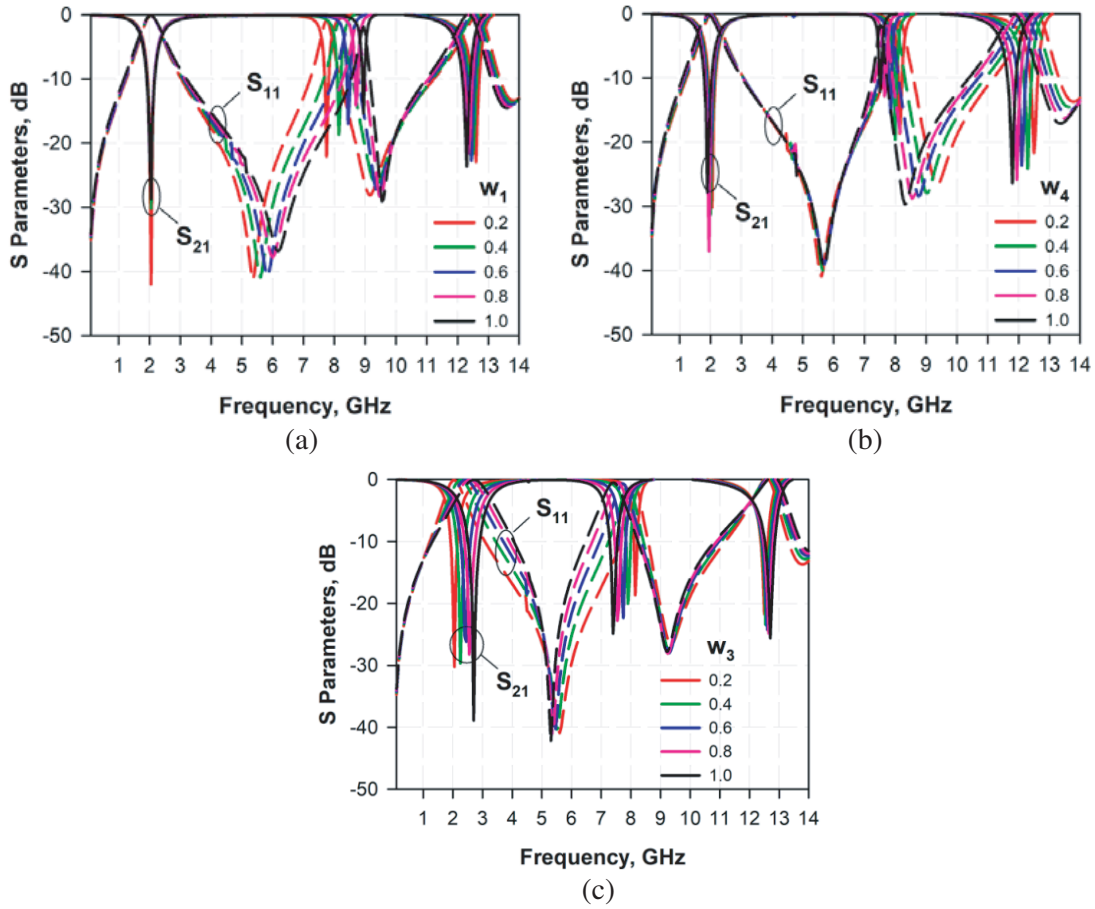


**Figure 2.** Effects of the changes in resonator widths on the frequency responses, (a)  $w_1$ , (b)  $w_4$ , (c)  $w_3$  (All in mm).

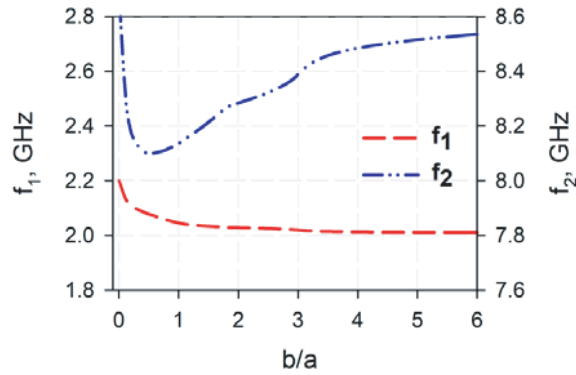


**Figure 3.** Investigation of resonance frequencies with respect to the change in  $b/a$ .

$a = 2.8$  mm,  $b = 3.0$  mm,  $w_1 = 0.4$  mm,  $w_2 = 0.9$  mm,  $w_3 = w_4 = 0.2$  mm,  $w_f = 1.9$  mm,  $t = 0.7$  mm,  $g_1 = 0.4$  mm and  $g_2 = 0.2$  mm,  $d_1 = 3.1$  mm and  $d_2 = 10.6$  mm. It should be noted that the gaps between the arms of the hairpin resonators are smaller than the single resonator shown in Fig. 1(a). Thus, there is a coupling between the transmission lines having widths of  $w_2$  and  $w_3$ . This is required for obtaining better performance in the second stopband. The coupling effect is demonstrated in Fig. 5. As can be seen from the figure, the return loss level can be dramatically improved by means of the

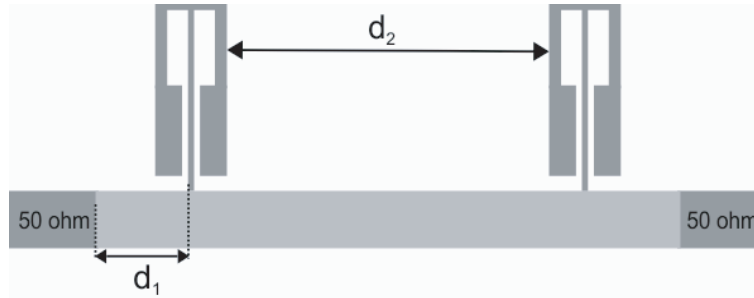


Figure 4. Dual-band bandstop filter structure.

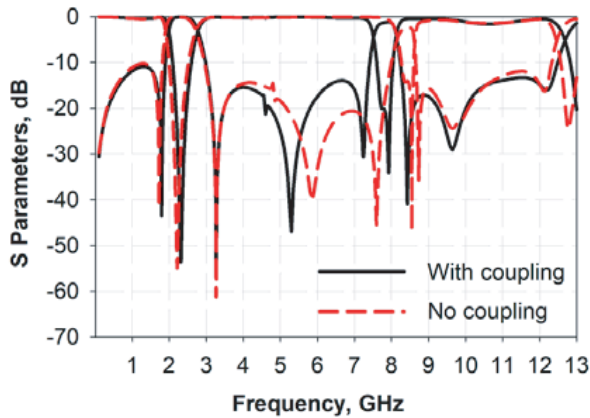


Figure 5. Effect of coupling between the arms of the hairpin resonator on the frequency response.

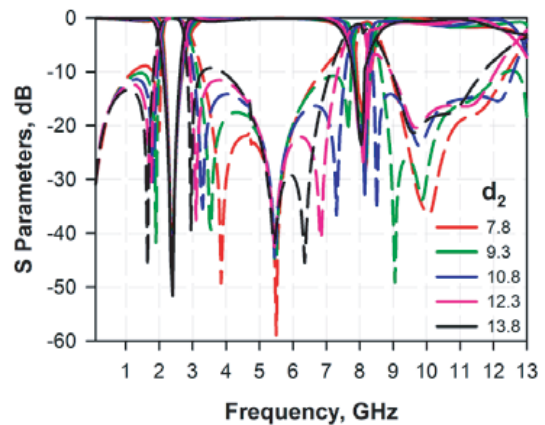


Figure 6. Effects of  $d_2$  on the frequency response (All in mm).

coupling effect. In Fig. 5, the frequency response called as no coupling can be obtained by increasing the gaps between the transmission lines having the widths of  $w_2$  and  $w_3$ , without changing the filter dimensions.

The distance between the resonators,  $d_2$ , is also effective on the frequency response as depicted in Fig. 6. As shown, bandwidths of the stopbands can be simultaneously controlled. During this change, return loss levels near the stopbands can be varied. At the same time, reflection zeros except the middle one can be moved. In addition, the reflection pole (transmission zero) of the first stopband is almost fixed, while the reflection poles in the second stopband move more. It is clear that the second stopband begins to deteriorate when  $d_2$  is greater than 9.3 mm.

Effects of the changes in  $a$  and  $b$  lengths of the hairpin resonators on the frequency response are represented in Figs. 7(a) and 7(b) for wideband and narrowband views, respectively. It should be noted that while  $a$  increases,  $b$  must be decreased. While  $a$  varies from 1.2 mm to 4.4 mm,  $b$  can be changed from 4.6 mm to 1.4 mm, respectively. These changes exhibit similar behaviour to the single resonator filter shown in Fig. 3. It is clear that only the second stopband can be controlled, while the first stopband is fixed. Control operation can only be achieved over the center frequency. Bandwidth and return loss levels inside the stopbands are almost unchanged. On the other hand, if only  $a$  is varied, both stopbands can be simultaneously controlled since the total electrical length of the filter is also changed. As can be seen from Fig. 8, while  $a$  increases, center frequencies of both stopbands can be decreased. However, some degradation also appears, especially in the passband return loss levels.

It should be noted that the filter design frequency is determined by the resonator dimensions. For a simple design procedure, firstly, the stopband frequencies must be decided and the resonator dimensions should be determined. The stopband frequencies can be adjusted by means of the approach described in the previous section. Figs. 2 and 3 can also be used for frequency assignment. In order to increase the selectivity of the stopbands, the second stepped impedance hairpin resonator is located at a distance of

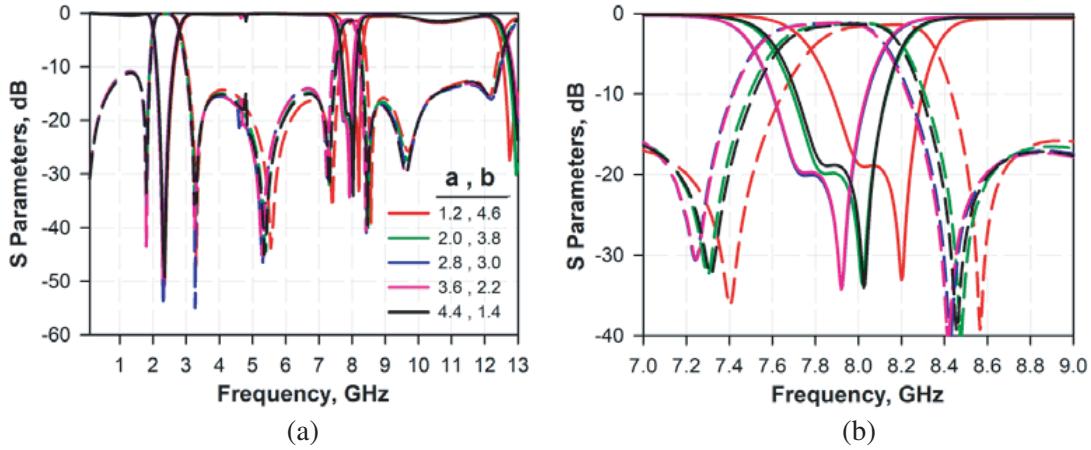


**Figure 7.** Effects of  $a$  and  $b$  changes on the frequency response, (a) wideband, (b) narrow band.

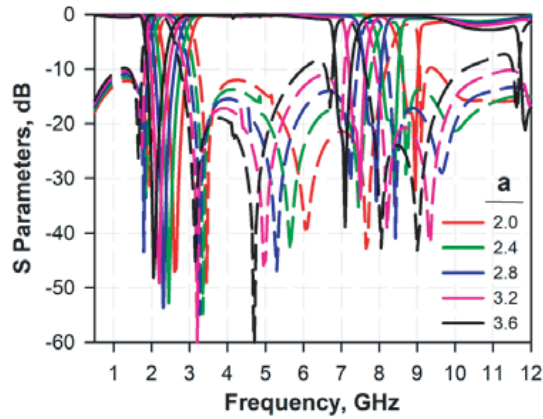


**Figure 8.** Effects of  $a$  on the frequency response.

$d_2$  along the main line. The distance  $d_2$  can be adjusted to obtain the desired bandwidth and insertion loss levels outside of the stopbands by an optimization. The effect of  $d_2$  on the frequency response is also demonstrated in Fig. 6. The final sensitive frequency adjustment can be realized according to Figs. 7 and 8.

#### 4. EXPERIMENTAL STUDIES

The proposed dual-band bandstop filter has been fabricated for the experimental verification of the predicted results. A photograph of the fabricated filter is shown in the inset of Fig. 9.  $50\ \Omega$  SMA connectors were used to measure the fabricated filter. Measurements have been performed by a Vector Network Analyzer HP8720C. Comparisons of the measured and simulated results are illustrated in Fig. 9. As can be seen from the figure, measured results exhibit an excellent agreement with the simulated results. Small differences between the simulated and measured results are due to the tolerances in the substrate, losses of SMA connectors and fabrication. In simulations, two stopbands centered at 2.34 GHz and 7.81 GHz with the fractional bandwidths of 33.2% and 7.9% have been obtained, respectively. In measurements, center frequencies of the stopbands have been obtained as 2.39 GHz and 7.82 GHz with the fractional bandwidths of 34.8% and 7.3%, respectively. The bandwidth of the passband between the stopbands is 5.47 GHz. So, the second stopband occurs at the center frequency of  $3.34f_1$  where  $f_1$  is the center frequency of the first stopband. However, the center frequency of the second band can be increased to approximately  $4.4f_1$  for the proposed filter, as shown in Fig. 2(a). This is the

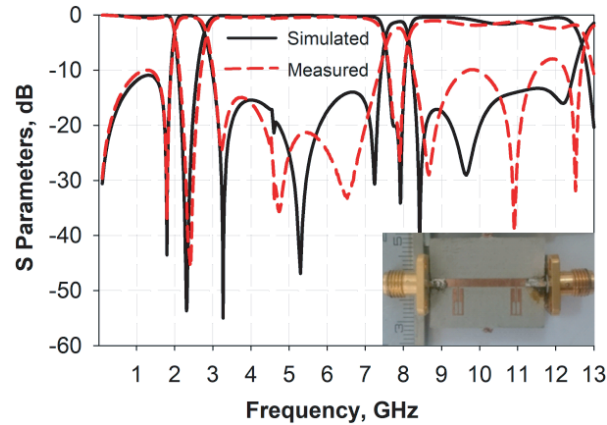


**Figure 9.** Comparison of the measured and simulated results (inset figure: Photograph of the fabricated filter).

most significant property of the filter proposed without using any harmonic suppression method such as defected ground structure, multilayer structure. Moreover, the simulated and measured return losses inside the stopbands are 0.07/1.16 dB and 0.41/2.36 dB for the first and second stopbands, respectively. In-band rejection levels have been measured as better than 45 dB and 18 dB for the first and second stopbands, respectively.

## 5. CONCLUSION

A new type of dual-band microstrip bandstop filter has been designed, fabricated, and tested. The designed filter has been formed by locating stepped impedance hairpin resonators to a simple straight transmission line. Detailed analyses of the filter have been achieved by investigating the circuit parameters. Measured results of the fabricated filter have exhibited an excellent agreement with the simulated ones.

The designed filter has promising advantages in terms of compact size, acceptable rejection levels, and measurement results. Since the designed filter provides two stopbands, it may be utilized in multifunction communication systems which require suppression of unwanted signals. The most significant advantage of the proposed structure is to allow a wide passband between the stopbands by means of a very simple and understandable topology. For the proposed bandstop filter, the center frequency of the second stopband can be increased up to approximately 4.4 times that of the first band. It is obvious that any harmonic suppression method such as defected ground structure, multilayer structure has not been used.

## REFERENCES

1. Ma, Z., K. Kikuchi, Y. Kobayashi, T. Anada, and G. Hagiwara, "Novel microstrip dual-band bandstop filter with controllable dual-stopband response," *2006 Asia-Pacific Microwave Conference*, 1174–1177, Yokohama, 2006.
2. Karpuz, C., A. K. Gorur, and M. Emur, "Quad-band microstrip bandstop filter design using dual-mode open loop resonators having thin film capacitors," *IEEE Microwave and Wireless Components Letters*, Vol. 26, No. 11, 873–875, Nov. 2016.
3. Karpuz, C., A. Gorur, E. Gunturkun, and A. K. Gorur, "Asymmetric response dual-mode dual-band bandstop filters having simple and understandable topology," *2009 Asia Pacific Microwave Conference*, 925–928, Singapore, 2009.
4. Gao, L., S. W. Cai, X. Y. Zhang, and Q. Xue, "Dual-band bandstop filter using open and short stub-loaded resonators," *2012 International Conference on Microwave and Millimeter Wave Technology (ICMMT)*, 1–3, Shenzhen, 2012.

5. Hsieh, L.-H. and K. Chang, "Compact lowpass filter using stepped impedance hairpin resonator," *Electronics Letters*, Vol. 37, No. 14, 899–900, Jul. 5, 2001.
6. Hsieh, L.-H. and K. Chang, "Compact elliptic-function low-pass filters using microstrip stepped-impedance hairpin resonators," *IEEE Transactions on Microwave Theory and Techniques*, Vol. 51, No. 1, 193–199, Jan. 2003.
7. Sagawa, M., K. Takahashi, and M. Makimoto, "Miniaturized hairpin resonator filters and their application to receiver front-end MICs," *IEEE Transactions on Microwave Theory and Techniques*, Vol. 37, No. 12, 1991–1997, Dec. 1989.
8. Wang, H. and Q. Chu, "A narrow-band hairpin-comb two-pole filter with source-load coupling," *IEEE Microwave and Wireless Components Letters*, Vol. 20, No. 7, 372–374, Jul. 2010.
9. Zhu, J. and Z. Feng, "Microstrip interdigital hairpin resonator with an optimal physical length," *IEEE Microwave and Wireless Components Letters*, Vol. 16, No. 12, 672–674, Dec. 2006.
10. Quevedo-Teruel, O., L. Inclán-Sánchez, J. Vazquez-Roy, and E. Rajo-Iglesias, "Compact reconfigurable planar EBGs based on short-circuited hairpin resonators," *IEEE Microwave and Wireless Components Letters*, Vol. 23, No. 9, 462–464, Sept. 2013.
11. Oraizi, H. and N. Azadi-Tinat, "Optimum design of novel UWB multilayer microstrip hairpin filters with harmonic suppression and impedance matching," *International Journal of Antennas and Propagation*, Vol. 2012, Article ID 762790, 7 pages, 2012.
12. Zhu, Y. Z., X. J. Zhang, and G. Y. Fang, "General design of compact T-shaped line filter with ultra-wide stopband," *PIERS Proceedings*, 1555–1558, Moscow, Russia, Aug. 18–21, 2009.
13. Kim, C.-S., T.-H. Lee, B. Shrestha, and K.-C. Son, "Stepped impedance resonator bandstop filter based on hairpin coupling configurations", *International Journal of Information Communication Technology and Digital Convergence*, Vol. 1, No. 1, 20–23, 2016.
14. Zhang, Y. H. and X. H. Tang, "Compact bandstop filter using novel coupled-line hairpin unit," *2015 IEEE International Conference on Communication Problem-Solving (ICCP)*, 66–68, Guilin, 2015.
15. Majidifar, S., S. V. A. Makki, S. Alirezaee, and A. Ahmadi, "Dual-band bandstop filter using modified stepped-impedance hairpin resonators," *2013 5th International Conference and Computational Intelligence and Communication Networks*, 61–63, Mathura, 2013.
16. *Sonnet User's Manual*, Version 16, Sonnet Software, North Syracuse, NY, 2016.